International Congress on Environmental Modelling and Software

5th International Congress on Environmental Modelling and Software - Ottawa, Ontario, Canada - July 2010

Jul 1st, 12:00 AM

The Impact of Climate Change on Agriculture Water Resources for Paddy Rice over Southern Taiwan

Pao-Shan Yu

Hung-Wei Tseng

Shien-Tsung Chen

Yu, Pao-Shan; Tseng, Hung-Wei; and Chen, Shien-Tsung, "The Impact of Climate Change on Agriculture Water Resources for Paddy Rice over Southern Taiwan" (2010). *International Congress on Environmental Modelling and Software*. 284.
https://scholarsarchive.byu.edu/iemssconference/2010/all/284

International Environmental Modelling and Software Society (iEMSs)
2010 International Congress on Environmental Modelling and Software
Modelling for Environment's Sake, Fifth Biennial Meeting, Ottawa, Canada
David A. Swayne, Wanhong Yang, A. A. Voinov, A. Rizzoli, T. Filatova (Eds.)
http://www.iemss.org/iemss2010/index.php?n=Main.Proceedings

The Impact of Climate Change on Agriculture Water Resources for Paddy Rice over Southern Taiwan

Pao-Shan Yu[a]*, Hung-Wei Tseng[a], Shien-Tsung Chen[a]
[a] *Department of Hydraulic and Ocean Engineering, National Cheng Kung University, Taiwan*
* yups@ncku.edu.tw

Abstract: This work aims to investigate the impacts of hydrologic drought on agricultural water resources under climate change scenarios. The study area is Tseng-Wen Reservoir basin in southern Taiwan, which receives temporally uneven precipitation. It is thus a basin prone to suffer from drought during dry season. General circulation models (GCMs) are the main tool to tackle climate change issues through the help of prescribed scenarios. This work used several approaches, including spatial downscaling, temporal downscaling and hydrologic model, to solve the coarse-resolution problem of GCMs and then to analyze the effect of climate change in the study area. The following are important findings: (1) According to future climate projections, droughts may become more frequent (hereafter referred to as scenario droughts), but their duration and magnitude may become more diverse than those of the baseline droughts. (2) The times of start and end of scenario droughts may occur earlier than those of baseline droughts. (3) Scenario low flow during the dry period tends to decrease in January and February, but to increase in March and April. (4) Moderate adjustment of irrigation period to adapt to climate change is suggested.

***Keywords**: climate change, downscaling methods, hydrologic drought.*

1. INTRODUCTION

Numerous investigations have studied rainfall trends in various areas worldwide and have found that rainfall characteristics vary according to regions, and have increasing or decreasing trends. Yu et al. [2006] found that annual rainfall in southern Taiwan has decreased significantly during the past century. This work investigated the hydrologic drought pertaining to streamflow in Tseng-Wen Reservoir basin in Taiwan under climate change scenarios. Droughts can be classified as meteorological drought, hydrologic drought and agricultural drought based on the question considered. The threshold level approach proposed by Yevjevich [1967] has been the most commonly applied approach to drought studies, such as Kjeldsen et al. [2000], Shiau et al. [2001], Hisdal et al. [2001], Shiau [2003], Fleig et al. [2006], and Shukla et al. [2008]. This work also defines a hydrologic drought event by using the threshold level approach and aims to investigate impacts of climate change on agricultural water resources in southern Taiwan, in which the temporal precipitation is very uneven. Around 90% of annual precipitation occurs during the period from May to October (wet period) but only 10% of annual precipitation occurs from December to April (dry period). Although there is less precipitation during the dry period, the temperature is more suitable for paddy rice growth. Recently, the shortage of water resource during the dry period always causes the paddy field to lie fallow. Whether the water resource distribution during this period is influenced by climate change in the future is our concern in this work. Tseng-Wen Reservoir, the major water resource for dry period in southern Taiwan, is chosen as the study area in this work.

2. STUDY AREA AND DATA SET

Tseng-Wen Reservoir, with a storage capacity of about 7.8×10^8 m^3, is the largest reservoir in Taiwan. Tseng-Wen Reservoir was completed in 1973, having multifunction of the water demands for agriculture, domestic use, flood control and hydropower generation. Tseng-Wen Reservoir basin encloses an area of 481 km^2 (Figure 1), and is at an elevation of from 157 to 3,514 m above sea level. The mean annual precipitation is about 2,740 mm, of which nearly 90% occurs during the wet season (Figure 1).

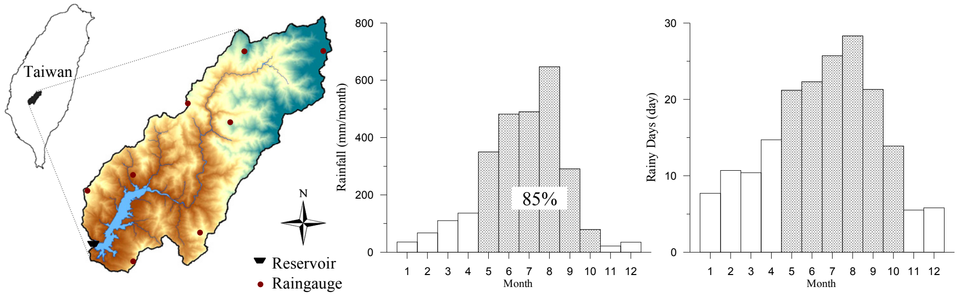

Figure 1. Tseng-Wen Reservoir basin (left); precipitation (center) and rainy days (right) over the basin.

Climate and hydrological data used in this work contain local-scale and large-scale data. Local-scale data, including precipitation, streamflow and temperature, are provided by Water Resource Agency, Taiwan. Long-term daily precipitations (1974−2008) are available from eight raingauges, from which areal precipitations on Tseng-Wen Reservoir basin were computed using the Thiessen polygon method. In this work, historical streamflow data are regarded as a datum, baseline, against which change is compared.

Large-scale data, i.e. general circulation models (GCMs) data, were downloaded from the Data Distribution Center of the United Nations Intergovernmental Panel on Climate Change.

The climate scenarios describe the emission conditions of green house gas and there are more details in IPCC [2007]. Different scenarios used were for historical climate (20C3M), and future climate (A1B and B1). Generally speaking, 20C3M is the scenario to represent past climate, A1B is regarded as the most likely climate scenario in the future and B1 describes a convergent world that the impact on climate change is slighter than A1B. The time periods of historical scenario and future scenario data are 1975−2000 and 2010−2045 respectively. Table 1 lists the summary of six adopted GCMs.

Table 1. Summary of the GCMs used in this work.

Model	Country	Resolution
CGCM3.1(T63)	Canada	T63,L31
ECHAM5/MPI-OM	Germany	T63,L31
CSIRO-Mk3.0	Australia	T63,L18
GFDL-CM2.0	U.S.A.	2°×2.5°,L24
GFDL-CM2.1	U.S.A.	2°×2.5°,L24
MIROC3.2(hires)	Japan	T106,L56

3. METHODOLOGY

3.1 Daily Rainfall Downscaling

GCMs are used as the main tool to project climate changes through the use of emission scenarios. However, due to the coarse resolution, GCMs are not able to represent regional topography and land-sea contrast properly, making local climate projection a big challenge. Thus a two-stage statistical downscaling method was applied to generate future daily precipitation data from climate outputs run by six GCMs. In the first stage, spatial statistical downscaling was applied by using the singular value decomposition (SVD) scheme (Chu, J.L. et al. [2008]) to downscale the monthly precipitation from six GCMs. In the second stage, the projected changes of monthly precipitation were further used in a weather generator to project the daily precipitation, as shown in Figure 2. Daily data are more practical for hydrological purpose. After the daily precipitation is generated, the hydrological model uses daily rainfall as an input to simulate daily streamflow.

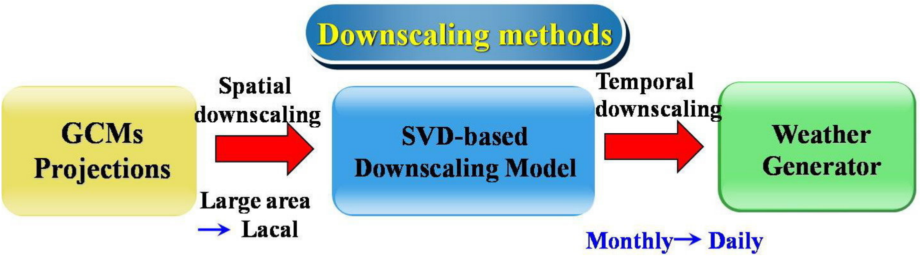

Figure 2. Two-stage statistical downscaling method.

3.1.1 Spatial Statistical Downscaling

Spatial statistical downscaling provides relationships between local and large-scale variables to overcome the drawback of GCMs' coarse-resolution. The first step of spatial downscaling is data reconstruction by the empirical orthogonal functions (EOFs) to filter off noises. This method is the same as principal components analysis. Then the SVD is applied to extract coupled patterns between local precipitation and large-scale variables. The analysis from SVD-based spatial statistical downscaling scheme shows that the rainfall over the study area is closely tied to the large-scale circulation over the east Asia monsoon region, and that GCMs perform reasonably well in simulating the mean states of sea level pressure (SLP) and meridional wind field at 850hPa (V850) over this region. Consequently, the two large-scale variables, SLP and V850, both of which are taken from six GCMs involving 20C3M, A1B, and B1 scenarios, are used as predictors for downscaling. After spatial downscaling process, the results from these scenarios are used to calculate the future change rates of precipitation. The change rates are the ratio of A1B to 20C3M and the ratio of B1 to 20C3M. Historical monthly rainfall multiplied by change ratios are future projections of monthly rainfall under A1B and B1 scenarios.

3.1.2 Temporal Statistical Downscaling

In the second stage, a stochastic weather model was applied to downscale the monthly precipitation, derived in the first stage, to daily precipitation (Figure 3). The daily precipitation generation is based on procedures proposed by Richardson [1981]. The generator uses a Markov chain to model the occurrence of wet or dry days, and a probability distribution to generate the precipitation amount conditional on a wet day modeled by the Markov chain. A first-order two-state Markov chain was used in this work. The occurrence of a dry or wet day is modeled by a transition probability matrix consisting of conditional probabilities, given a previous dry or wet day.

Many probability distributions were applied to generate daily precipitation amount, such as the exponential distribution (Selker et al. [1990]; Tung et al. [1995]), Weibull distribution (Yu et al. [2002]), two-parameter gamma distribution (Richardson [1981]; Coe et al. [1982]; Woolhiser et al. [1982]; Schubert [1994]; Corte-Real et al. [1999]), and mixed exponential distribution (Woolhiser et al. [1979]; Woolhiser et al. [1982] [1986]). Among the probability distributions, the Weibull distribution approximates daily rainfall in Taiwan the best (Yu et al. [2002]); consequently, it was used to generate daily rainfall.

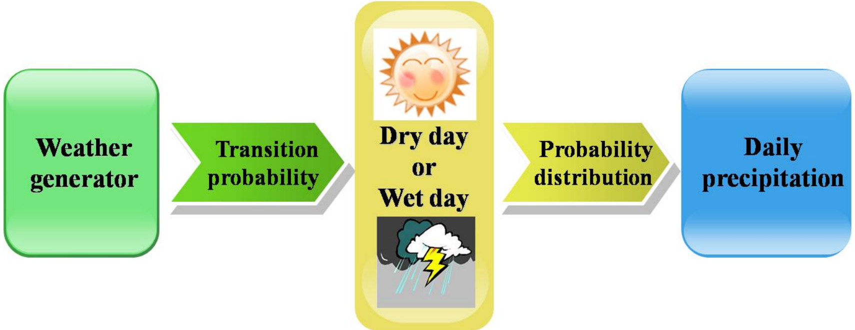

Figure 3. The temporal downscaling process (weather generator).

3.2 Hydrological Model

A continuous hydrologic model was needed to simulate future projected streamflow, after the daily precipitation under the A1B and B1 scenarios were obtained in the previous section by the downscaling. This work used a continuous hydrologic model based on the structure of Hydrologiska Byråns Vattenbalansavdelning (HBV) model (Bergström [1976] [1992]), which was initially designed for use in Scandinavian catchments by the Swedish meteorological and hydrological institute. Yu and Yang [2000] adapted the HBV model structure to suit catchments in Taiwan. The modified HBV model uses both an upper and lower tanks to model the rainfall-runoff behavior. Model structure mainly consists of three parts: (1) soil moisture module, (2) runoff response mechanism, and (3) water balance functions. Detail description of the modified HBV model, as well as its calibration and validation in this work, can be found in Yu and Yang [2000] and Yu et al. [2002].Historical daily rainfall and flow data from 1975 to 1998 were used for model calibration. The calibrated continuous hydrologic model was further verified by historical data from 1999 to 2008. The results from this work found the continuous hydrologic model to be able to simulate the rainfall-runoff behavior over the study area.

3.3 Hydrological Drought Event

The threshold level method is applied to define a drought event. In order to study the features of major hydrological drought, this work defines a hydrologic drought as a low flow event when streamflow series is continuously below Q_{50} (50% probability of exceedance) and the minimum flow during the period is less than Q_{90} (Figure 4). The Q_{90} is required here to avoid minor drought events. Once a drought event is specified, drought characteristic can be quantified. Drought frequency [time/year] is the times of drought occurrence per year. Drought duration [day] is the time period between drought start and end. Drought magnitude [mm] is the total amount of streamflow deficit, expressed in depth. Moreover, to avoid the dependent droughts and slight droughts, a 7-day moving average is used to preprocess the simulated streamflow data.

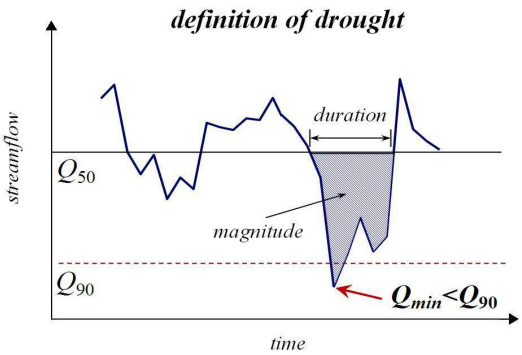

Figure 4. Definition of drought.

4. RESULTS AND DISCUSSION

In following discussion, projected data are in view of the most likely scenario (A1B) and oncoming time period (2010−2045). By comparing differences between historical data (baseline) and projected data, the impact of climate change can be assessed. Table 2 shows drought characteristics, including drought frequency, duration, magnitude, based on historical data (baseline) and projected data (results from GCMs under A1B scenario). The scenario droughts exhibit a more frequent trend (0.87~1.02 times per year, the minimum and maximum of the GCMs, respectively.), compared with the frequency of baseline droughts (0.77 times per year). The durations of projected droughts are between 132 days and 193 days, and the magnitudes of projected droughts are between 105 mm and 179 mm. The duration and magnitude of scenario droughts maybe increase or decrease, as they depend on GCMs. Overall, scenario hydrological droughts may become more frequent, but their duration and magnitude may become more diverse than the baseline droughts.

Table 2. Impact of climate change on hydrologic drought

Model	Frequency (time/year)	Duration (day)	Magnitude (mm)
Baseline	0.77	174	148
CGCM3.1(T63)	0.87	132	105
ECHAM5/MPI-OM	0.99	159	137
CSIRO-Mk3.0	1.02	193	179
GFDL-CM2.0	0.98	182	165
GFDL-CM2.1	0.89	150	126
MIROC3.2(hires)	0.90	152	127
Model average	0.94	161	140

Figures 5 and 6 are the time distributions of start and end of scenario droughts respectively. In the figures, the solid line indicates the baseline drought, and the dash line stands for the scenario droughts, which is the ensemble mean of GCMs. Figure 5 indicates that baseline droughts may occur during the period from mid-October (2nd 10-day period of October) to early November (1st 10-day period of November). However, there is a single-peak form in scenario droughts. Relative to historical data, scenario droughts come early and concentrate in mid-October (2nd 10-day period of October). Figure 6 reveals that scenario droughts may end earlier than baseline droughts ending in early May (1st 10-day period of May). Generally speaking, drought may start and end earlier in the future.

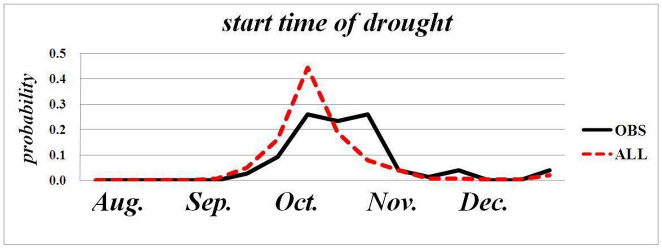

Figure 5. Distribution of drought start time.

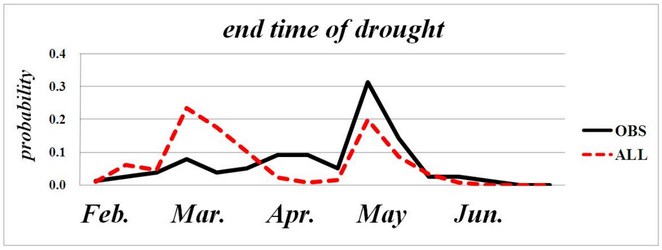

Figure 6. Distribution of drought end time.

Figure 7 presents the distribution of streamflow during the dry period. Solid lines and dash lines represent baseline drought and scenario drought respectively. For solid lines, the upper is 95th percentile, the lower is 5th percentile and the line in bold is median (50th percentile). The same notation is used for baseline data (dash lines). The scenario flow, which is derived from the ensemble average of GCMs, tends to decrease in January and February (at the beginning of paddy rice growth season) but to increase in March and April (at the end of paddy rice growth season). The 90% confidence interval of scenario flow is wider than baseline flow after February, indicating the future projected flow is more diverse.

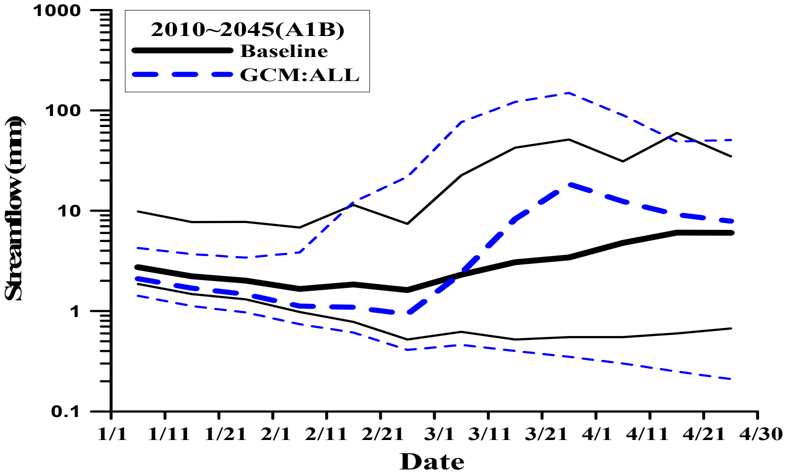

Figure 7. Streamflow distribution during dry season

5. CONCLUSIONS

This work successfully applied downscaling methods and a hydrological model to assess the effect of climate change on agriculture water resources in southern Taiwan. The results of drought characteristics indicate that scenario droughts may become more frequent, but their duration and magnitude may become more diverse than the baseline droughts. Analyzing time distributions of scenario drought finds that 10-day streamflow patterns are changed during the period of paddy rice growth. Generally speaking, drought event will start and end earlier in the future. The scenario flow trends to decrease in January and February (at the beginning of paddy rice growth season) but to increase in March and April (at the end of paddy rice growth season). The 90% confidence interval of scenario flow is wider than baseline flow after February, because diverse property of future flow is projected. Due to the changed pattern of streamflow, moderate adjustment of irrigation period to adapt to climate change is suggested.

ACKNOWLEDGMENTS

The authors would like to thank the National Science Council of the Republic of China (Taiwan) for financially supporting this research under Contract No. NSC 97-2625-M-006-014.

REFERENCES

Bergström, S., Development and application of a conceptual runoff model for Scandinavian Catchments, SMHI, Reports RHO. 7, Norrköping., 1976.

Bergström, S., The HBV model–its structure and applications, SMHI, Reports RHO. 4, Norrköping, 1992.

Chu, J.L., H. Kang, C.Y. Tam, C.K. Park, and C.T. Chen, Seasonal forecast for local precipitation over northern Taiwan using statistical downscaling. *Journal of Geophysical Research*, 113, D12118, 2008.

Coe, R., and R.D. Stern, Fitting models to rainfall data. *Journal Applied Meteorology*, 21, 1024–1031, 1982.

Corte-Real, J., H. Xu, and B. Qian, A weather generator for obtaining daily precipitation scenarios based on circulation patterns, *Climate Research*, 13, 61–75, 1999.

Fleig, A.K., A.K. Tallak Fleig, L.M., Tallaksen, H., Hisdal, and S. Demuth, A global evaluation of streamflow drought, *Hydrology and Earth System Sciences*, 10, 535–552, 2006.

Hisdal, H., K. Stahl, L.M. Tallaksen, and S. Demuth, Have streamflow droughts in Europe become more severe and frequent, *International Journal of Climatology*, 21, 317–333, 2001.

IPCC, Climate change 2007: the physical science basis, *The Fourth Assessment Report*, 2007.

Kjeldsen, T.R., A. Lundorf, and D. Rosbjerg, Use of a two-component exponential distribution in partial duration modeling of hydrological droughts in Zimbabwean rivers, *Hydrological Sciences Journal*, 15(2), 185–298, 2000.

Richardson, C.W., Stochastic simulation of daily precipitation, temperature, and solar radiation. *Water Resources Research*, 17, 182–190, 1981.

Schubert, S., A weather generator based on the European 'Grosswetterlagen', *Climate Research*, 4, 191–202, 1994.

Selker, J.S., and D.A. Haith, Development and testing of single-parameter precipitation distributions, *Water Resources Research*, 26(11), 2733–2740, 1990.

Shiau, J. T., and H.W. Shen, Recurrence analysis of hydrological droughts of differing severity, *Journal of Water Resources Planning and Management*, 127(1), 30–40, 2001.

Shiau, J. T., Return period of bivariate distributed extreme hydrological events. *Stochastic Environmental Research and Risk Assessment*, 17, 42–57, 2003.

Shukla, S., and A.W. Wood, Use of a standardized runoff index for characterizing hydrologic drought, *Geophysical Research Letters*, 35, L02405, 2008.

Tung, C.P., and D.A. Haith, Global-warming effects on New York streamflows, *Journal of Water Resources Planning and Management*, 121(2), 216–225, 1995.

Woolhiser, D.A., and G.G.S. Pegram, Maximum likelihood estimation of fourier coefficients to describe seasonal variation of parameters in stochastic daily precipitation models, *Journal Applied Meteorology*, 18, 34–42, 1979.

Woolhiser, D.A., and J. Roldan, Seasonal and regional variability of parameters for stochastic daily precipitation models, *Water Resources Research*, 22, 965–978, 1986.

Woolhiser, D.A., and J. Roldan, Stochastic daily precipitation models, 2. A comparison of distribution of amounts. *Water Resources Research*, 18, 1461–1468, 1982.

Yevjevich, V., An objective approach to definition and investigations of continental hydrologic droughts, Hydrology Paper 23, Colorado State University, Fort Collins, USA, 1967.

Yu, P. S., T.C. Yang, and C.C. Kuo, Evaluating long-term trends in annual and seasonal precipitation in Taiwan, *Water Resources Management,* 20**,** 1007–1023, 2006.

Yu, P.S., and T.C. Yang, Fuzzy multi-objective function for rainfall-runoff model calibration. *Journal of Hydrology*, 238(1-2), 1–14, 2000.

Yu, P.S., T.C. Yang, and C.K. Wu, Impact of climate change on water resources in southern Taiwan. *Journal of Hydrology*, 260(1–4), 161–175, 2002.